Korean J. Chem. Eng., **29**(9), 1115-1118 (2012)
DOI: 10.1007/s11814-012-0033-0

RAPID COMMUNICATION

A study of the palladium size effect on the direct synthesis of hydrogen peroxide from hydrogen and oxygen using highly uniform palladium nanoparticles supported on carbon

Youngjin Ye*,‡, Jinyoung Chun*,‡, Sunyoung Park, Tae Jin Kim***, Young-Min Chung***, Seung-Hoon Oh***, In Kyu Song**, and Jinwoo Lee*,†**

*Department of Chemical Engineering, Pohang University of Science and Technology, Pohang 790-784, Korea
**School of Chemical Biological Engineering, Institute of Chemical Processes, Seoul National University, Seoul 151-744, Korea
***Catalyst Lab, Catalyst & Process R&D Center, Global Technology, SK Innovation, Daejeon 305-712, Korea
(*Received 7 February 2012 • accepted 8 March 2012*)

Abstract–Highly monodisperse carbon-supported palladium nanoparticles with controllable size (3 nm, 6.5 nm, 9.5 nm) were prepared using a simple colloidal method, and the size dependence of the catalytic performance for the direct synthesis of hydrogen peroxide from hydrogen and oxygen was studied. Smaller-sized supported palladium nanoparticles showed both higher conversion of hydrogen and selectivity for hydrogen peroxide, compared to larger-sized supported particles. Among the catalysts tested, 3-nm Pd nanoparticles supported on carbon showed the highest yield for hydrogen peroxide because of the small size and high crystallinity.

Key words: Direct Synthesis of Hydrogen Peroxide, Hydrogen Peroxide, Palladium, Nanoparticles

INTRODUCTION

Hydrogen peroxide (H_2O_2) is a clean and strong oxidizing agent commonly used as a pulp/paper bleaching agent, which is of high industrial importance [1]. For example, more than 50% of H_2O_2 is used as a pulp/paper bleaching agent among the 2.2 metric tons of the annual production [2,3]. In addition to the pulp/paper bleaching, H_2O_2 has been used in wide range of applications such as textile bleaching, wastewater treatment, and desulfurization [1,4]. It is expected that the demand for H_2O_2 would have increased due to the increasing demand in new applications such as propylene oxide synthesis, in addition to the demand in conventional applications, including bleaching [3].

H_2O_2 has been conventionally produced by the so-called anthraquinone process, which was first developed by Riedl and Pfleiderer [5]. Over than 95% of the H_2O_2 has been produced by the anthraqunone process since the high-yield production of H_2O_2 is possible at mild temperatures without direct contact of hydrogen and oxygen gases [1]. Despite these advantages, however, the demand for a new method has increased because anthraquinone process suffers from the large amount of byproducts in wastewater and high energy consumption in the distillation of H_2O_2 [3].

Direct synthesis of H_2O_2 from H_2 and O_2 has been emerging as an alternative route, replacing the anthraquinone process [1,3]. This method is advantageous because it does not give large amount of wastewater compared to anthraquinone process, and it also does not need a bulky hydrogen carrier [6]. The direct route, therefore, is a much greener method for synthesis of H_2O_2. However, for industrial use there are two main obstacles to achieving direct synthesis of H_2O_2. First, mixtures of hydrogen and oxygen are explosive over a large range of concentration. Precise control of stoichiometry of reactant gases is necessary, in addition to dilution of gases by nitrogen, argon, or carbon dioxide [1]. Thanks to the extensive research on direct synthesis of H_2O_2, the safe conditions without explosion have been found in many patents [3]. Second, achieving high selectivity for hydrogen peroxide is very difficult because active catalysts for the direct synthesis of H_2O_2 have high activity for the combustion of hydrogen to water and further decomposition and hydrogenation of hydrogen peroxide [6,7].

Supported palladium (Pd) nanoparticles (NPs) have been found to be the most selective catalysts for direct synthesis of H_2O_2 [3]. The general strategies for improving the selectivity for hydrogen peroxide are alloying with Au or Pt [8-10], controlling the shape of NPs with desired exposed facets [11,12]. Although high selectivity over than 90% has been achieved with these methods [8,12], the origin of the high selectivity is still unclear. Identifying which factors might enhance the H_2O_2 selectivity has significant importance in design of highly selective catalysts.

The effect of particle size on selectivity in various catalytic reactions is critical in catalysis because important properties of particles in catalytic reactions such as exposed facets and surface-to-volume ratio are highly dependent on particle size [13-16]. Despite the significance of the study on the size dependent H_2O_2 selectivity, only a few studies have been reported [17]. The most probable reason is the difficulty of the synthesis of uniform Pd nanoparticles with controllable size. The recent advances in synthesis of nanoparticles have made it possible to control the size of nanoparticles with very high mono-dispersity [18-20]. Achieving high selectivity via using small and uniform-sized Pd nanoparticles was recently reported with the help of the development in monodispersed nanoparticle synthetic

†To whom correspondence should be addressed.
E-mail: jinwoo03@postech.ac.kr
‡These authors are equally contributed to this work.

techniques employing colloidal method [21].

In this paper, the size effect of Pd nanoparticles on direct synthesis of H_2O_2 was studied. Three different-sized Pd nanoparticles with high monodispersity were synthesized through the colloidal synthetic method. Direct synthesis of H_2O_2 was performed over 3-nm, 6.5-nm, 9.5-nm Pd nanoparticles supported on carbon black (Pd/C), and 3-nm Pd/C exhibited both the highest yield and selectivity for H_2O_2 among three catalysts. We expect that these results will provide insights into the design of highly active and selective catalysts for direct synthesis of H_2O_2.

EXPERIMENTAL SECTION

1. Materials

Palladium acetylacetonate ($Pd(acac)_2$, 99%), trioctylphosphine (TOP, tech. 90%), oleylamine (OAm, tech. 70%), toluene (99.8%) and ethanol (absolute, >99.8%) were purchased from Sigma-Aldrich. All chemicals were used without further purification.

2. Catalyst Preparation and Characterization

For the preparation of the Pd/C catalysts, we first synthesized Pd NPs [22] and they were deposited on carbon black [21] following previous reported methods.

2-1. 3-nm, 6.5-nm, 9.5-nm Pd NP Synthesis

For 3-nm Pd synthesis, we first prepared the Pd-trioctylphosphine (Pd-TOP) complex by dissolving 0.1 g of $Pd(acac)_2$ in 1 ml of TOP, and this solution was injected into the 9 ml of TOP. The mixed solution was heated to 300 °C for 30 min at 3 °C/min. All the procedures were performed under Ar atmosphere. After cooling to room temperature (RT), the black product was centrifuged down after adding absolute ethanol. The NPs were then redispersed in toluene for further use and characterization.

To obtain 6.5-nm Pd NPs, the solution of 0.1 g of $Pd(acac)_2$ dissolved in TOP 1 ml was injected into the 10 ml of oleylamine (OAm). The mixed solution was heated to 250 °C for 30 min at 3 °C/min. All the procedures were performed under Ar atmosphere. After the solution was cooled to RT, the 6 nm NPs were centrifuged down and redispersed in toluene.

For 9.5-nm Pd NP synthesis, we followed the same procedure for 6.5-nm Pd NP synthesis, except that TOP 0.15 ml was used for preparing Pd-TOP complex.

2-2. Preparation of Pd/C Catalysts

To prepare Pd/C catalysts, the desired amount of Pd NP was added into dispersed carbon black (Vulcan XC-72) in toluene and stirred for 24 h. The resultant Pd/C catalysts were collected by centrifugation. Total amount of deposited Pd NPs was characterized by ICP-AES technique.

2-3. Material Characterization

Transmission electron microscopy (TEM) images were taken on a JEOL JEM 1011 microscope. High-resolution TEM (HRTEM) images were taken on a JEOL JEM 2200 FS microscope with Image Cs-corrector.

3. Direct Synthesis of Hydrogen Peroxide

For the direct synthesis of hydrogen peroxide from hydrogen and oxygen, 1.0 g of each Pd/C catalyst and 80 ml of methanol were charged into the autoclave reactor. Sulfuric acid and sodium bromide were added as additives, and the concentrations of additives were 500 ppm of H_2O_4 and 100 ppm of NaBr, respectively. The mixed solution was vigorously stirred (1,000 rpm) with the bubbling of H_2/N_2 (25 mol% H_2) gas and O_2/N_2 (50 mol% O_2) gas. Total feed rate was maintained at 44 ml/min, while the H_2/O_2 ratio was fixed at 0.4. Catalytic reaction was carried out at 28 °C of temperature and 10 atm of pressure for 6 h. After the reaction, gas chromatograph (Younglin, ACME 6000) equipped with a TCD was used for an analysis of unreacted species, and iodometric titration method was used for determining the concentration of hydrogen peroxide. H_2 conversion, H_2O_2 selectivity and H_2O_2 yield were calculated using following equations.

$$H_2 \text{ conversion } (\%) = \frac{H_2 \text{ reacted (mol)}}{H_2 \text{ supplied (mol)}}$$

$$H_2O_2 \text{ selectivity } (\%) = \frac{H_2O_2 \text{ formed (mol)}}{H_2 \text{ reacted (mol)}}$$

$$H_2O_2 \text{ yield } (\%) = (H_2 \text{ conversion}) \times (H_2O_2 \text{ selectivity})$$

RESULTS AND DISCUSSION

1. Catalyst Characterization

To see the Pd size effect on direct synthesis of H_2O_2 from H_2 and O_2 clearly, we adopted the method for synthesis of highly uniform

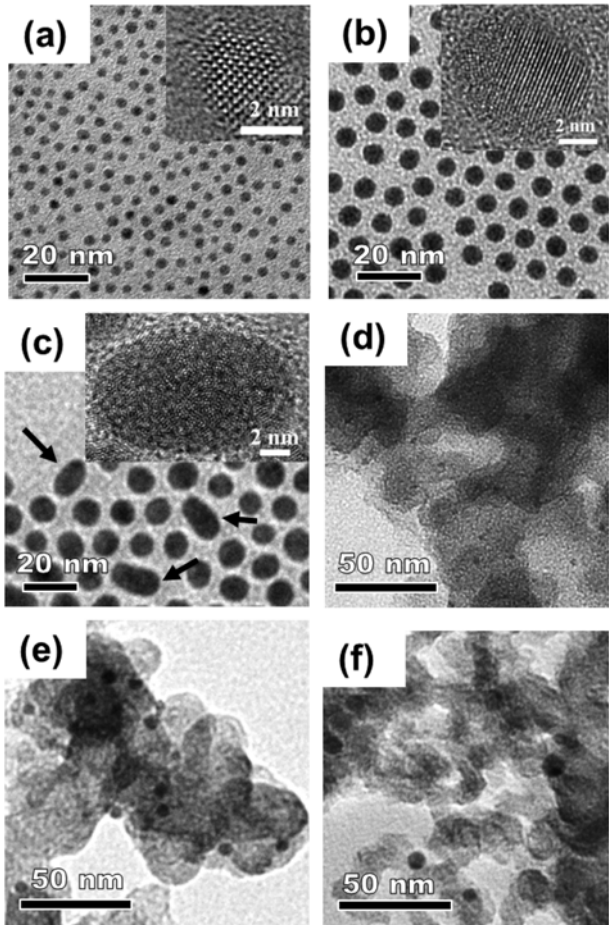

Fig. 1. TEM images of Pd NPs with the average size of (a) 3 nm, (b) 6.5 nm, and (c) 9.5 nm, respectively, and those of (d) 3-nm Pd/C, (e) 6.5-nm Pd/C, (f) 9.5-nm Pd/C. Insets in (a)-(c) indicate the high resolution TEM images. In (c), arrows indicate the irregular shaped Pd NPs.

Pd NPs [22]. Synthesis of monodisperse NPs allows us to analyze the size effect more accurately, in contrast to the analysis of that effect using NPs with high polydispersity. As shown in Fig. 1(a)-(c), TEM images of as-synthesized NPs revealed that highly uniform Pd NPs were obtained. The size distribution obtained by measuring the size of 100 particles for each sample also confirmed that Pd NPs were nearly monodisperse, except the 9.5-nm Pd NPs. Standard deviations were 11.7%, 6.1%, and 20.5% for NPs with the diameters of 3, 6.5, 9.5 nm, respectively.

For further investigation, HRTEM images were obtained (Fig. 1(a)-(c)). HRTEM images revealed that 3-nm and 6.5-nm Pd NPs have relatively higher crystallinity to show polycrystalline nature of Pd NPs. As opposed to the 3-nm and 6.5-nm NPs, 9.5-nm Pd NPs have oval shape and the surface is smooth to show relatively lower crystallinity.

3-nm Pd NPs were synthesized via thermal decomposition of a Pd-TOP complex in TOP (Fig. 1(a)). The sizes of Pd NPs were modulated by using the different binding strength of TOP and OAm. Since the binding strength of TOP is higher than OAm [22,23], 6.5-nm Pd NPs were synthesized when Pd-TOP complex was decomposed in OAm (Fig. 1(b)). If smaller amount of TOP was used to form Pd-TOP complex, 9.5-nm Pd NPs were obtained (Fig. 1(c)). In contrast to the 3-nm and 6.5-nm Pd NPs, 9.5-nm Pd NPs showed relatively broad size distribution with the larger standard deviation (20.5%), and irregular shaped NPs were also found. The broad size distribution of 9.5-nm Pd NPs is due to the relatively weaker binding strength of OAm than that of TOP. As the TOP ligands on Pd NPs are exchanged with OAm during the thermal decomposition, the reaction would give irregular shaped Pd NPs with broad size distribution.

To be used as catalysts for direct synthesis of H_2O_2, as-synthesized Pd NPs were deposited on carbon black (Vulcan XC-72). Pd NPs were easily impregnated on carbon by mixing the solution containing Pd NPs and carbon black [21]. TEM images of Pd/C revealed that Pd NPs were well-dispersed on carbon black without agglomeration. The Pd loadings were 0.35 wt% for 3-nm Pd/C, 0.73 wt% for 6.5-nm Pd/C, and 0.40 wt% for 9.5-nm Pd/C, respectively. The amount of Pd loading was intentionally kept low to avoid transport limitations [21]. This method is suitable for studying the size effect of Pd NPs due to the simplicity of catalysts preparation without affecting the size distributions of as-synthesized Pd NPs.

2. Direct Synthesis of H_2O_2

As noted in the introduction, the sizes of Pd NPs have a significant effect on the catalytic behavior of Pd/C catalysts in the direct formation of H_2O_2 from H_2 and O_2. Bromide ions and H_2SO_4 were added as additives to increase the productivity and selectivity for H_2O_2. It has been well known that addition of acid additives suppresses the decomposition of H_2O_2, thus leading to the increase in H_2O_2 selectivity [24]. In addition, bromide ions have been typically added in the reaction, mainly due to the increased productivity of H_2O_2 in the presence of halide ions [3]. Since the focus of this work is to study the Pd size effect for H_2O_2 synthesis, reaction conditions were kept the same for all experiments. The catalytic performance of Pd/C catalysts, after 6 hours of reaction, is shown in Fig. 2. As the size of Pd NPs decreases, H_2 conversion, H_2O_2 selectivity, and H_2O_2 yield increase. H_2O_2 yields over prepared catalysts were 16.2% for 3-nm Pd/C, 11.0% for 6.5-nm Pd/C, and 1.8% for 9.5-nm Pd/C, respectively. It is remarkable that 9.5-nm Pd/C catalysts showed

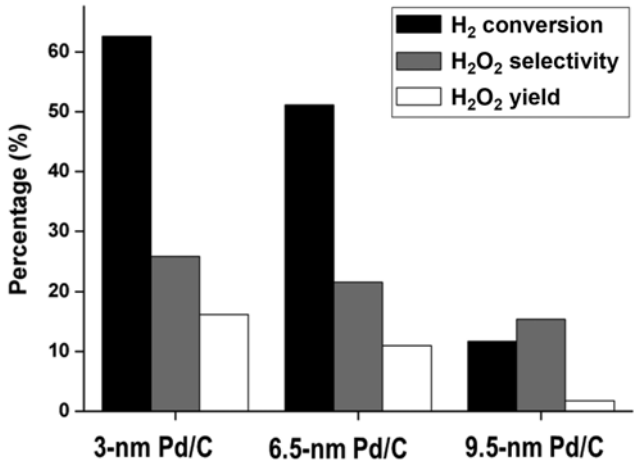

Fig. 2. Catalytic performance for direct synthesis of H_2O_2 from H_2 and O_2 over the Pd/C catalysts.

extremely low yield of H_2O_2 due to the very poor H_2 conversion over 9.5-nm Pd/C catalysts, compared to those of 3-nm and 6.5-nm Pd/C catalysts. Poor dispersion due to the relatively larger particle size of 9.5-nm Pd/C catalysts might be the reason for such a low H_2 conversion. In addition, 9.5-nm Pd/C catalysts showed the lowest H_2O_2 selectivity, which would be due to the irregular shape of catalysts (Fig. 1(c)). For selective catalysts in direct route to H_2O_2, Pd NPs should have regular shape without many defects because highly energetic sites including steps, kinks, and corners promote not only the formation of H_2O instead of H_2O_2 but also the decomposition of H_2O_2 [25,26]. From this point of view, the highest H_2 conversion and H_2O_2 selectivity over 3-nm Pd/C catalysts seem reasonable. It is noteworthy that 3.6-nm Pd NPs used in a previous report and 3-nm Pd NPs used in this work were both synthesized using the TOP ligands. On the other hand, 6.5-nm Pd NPs and 9.5-nm Pd NPs used in this work were synthesized using both TOP and OAm ligands. Therefore, use of only the TOP ligand might also be attributed to the high H_2 conversion and high H_2O_2 selectivity of 3-nm Pd/C.

The result obtained from the experiment is consistent with previous observation that the monodisperse 3.6-nm Pd NPs supported on carbon are more active in the formation of H_2O_2 compared to the larger Pd/C with the broader size distribution [21]. They insisted that high exposure of the (110) planes of 3.6-nm Pd NPs might promote the dissociative adsorption of H_2 and suppress the dissociation of O_2 and thus direct formation of H_2O_2 over 3.6-nm Pd NP/C is more facilitated.

This result, however, is opposed to the report by Centi et al. that 8-nm Pd NPs are most active among the 4-nm Pd NPs, 8-nm Pd NPs, and 16-nm Pd NPs supported on carbon-coated membranes [17]. They used H_2 reduction method to synthesize Pd NPs on membranes. According to them, either smaller (4-5 nm) or larger (15-16 nm) particles are not suitable as catalysts for direct synthesis of H_2O_2 because, as discussed above, they have highly energetic sites facilitating the formation of H_2O and decomposition of H_2O_2. Since the work reported by Centi et al. used Pd NPs synthesized by the H_2 reduction method, optimum size would be different from the work studied with Pd NPs synthesized by colloidal methods. It is

reasonable to assume that optimum size discrepancy between our work and work by Centi et al. can be attributed to the different synthetic condition.

The previous reports, despite these inconsistencies, give clear insights into the roles of size effect of Pd NPs on the direct synthesis of H_2O_2 from H_2 and O_2 [3]. Small (<4 nm) Pd NPs with high crystallinity without many defects can be synthesized using the colloidal methods, which is difficult to be obtained by H_2 reduction. Small Pd NPs synthesized by H_2 reduction might have many defects, thus causing the decrease of the H_2O_2 selectivity. On the other hand, monodisperse small Pd NPs with high crystallinity give the high H_2O_2 selectivity because of the small size and large surface-to-volume ratio. Therefore, to synthesize the small Pd NPs with high crystallinity would be the effective way to design the highly selective Pd catalysts in direct synthesis of H_2O_2 from H_2 and O_2.

CONCLUSIONS

A simple method for synthesizing highly monodisperse Pd NPs was adopted to study the size effect of Pd NPs in direct synthesis of H_2O_2 from H_2 and O_2. With this method, 3-nm, 6.5-nm, and 9.5-nm Pd/C with narrow size distributions have been synthesized successfully, and the size effect on direct formation of H_2O_2 was studied. Our results suggest that the synthesis of the smaller Pd catalysts with high crystallinity would be the key factor to increase the H_2O_2 selectivity. We expect that these results can be applied to the design of highly selective catalysts for direct synthesis of H_2O_2.

ACKNOWLEDGEMENTS

This research was supported by a grant from the Industrial Source Technology Development Programs (10033093) of the Ministry of Knowledge Economy (MKE) of Korea.

REFERENCES

1. J. M. Campos-Martin, G. Blanco-Brieva and J. L. G. Fierro, *Angew. Chem. Int. Ed.*, **45**, 6962 (2006).
2. R. Hage and A. Lienke, *Angew. Chem. Int. Ed.*, **45**, 206 (2006).
3. G. Centi, S. Perathoner and S. Abate, in *Modern heterogeneous oxidation catalysis: design, rections and characterization*, N. Mizuno Eds., Wiley-Verlag GmbH & Co. KGaA (2009).
4. K. Kosaka, H. Yamada, K. Shishida, S. Echigo, R. A. Minear, H. Tsuno and S. Matsui, *Water Res.*, **35**, 3587 (2001).
5. H.-J. Riedl and G. Pfleiderer, US Patent, 2,158,525 (1939).
6. J. K. Edwards and G. J. Hutchings, *Angew. Chem. Int. Ed.*, **47**, 9192 (2008).
7. S. Park, T. J. Kim, Y.-M. Chung, S.-H. Oh and I. K. Song, *Korean J. Chem. Eng.*, **28**, 1359 (2011).
8. J. K. Edwards and B. Solsona, *Science*, **323**, 1037 (2009).
9. S. Abate, S. Melada, G. Centi, S. Perathoner, F. Pinna and G. Strukul, *Catal. Today*, **117**, 193 (2006).
10. J. K. Edwards, B. Solsona, P. Landon, A. F. Carley, A. Herzing, C. J. Kiely and G. J. Hutchings, *J. Catal.*, **236**, 69 (2005).
11. Z. Zhou, Z. Wu, C. Zhang and B. Zhou, US Patent, 7,601,668 (2009).
12. B. Zhou and L.-K. Lee, US Patent, 6,168,775 (2001).
13. G. A. Somorjai, H. Frei and J. Y. Park, *J. Am. Chem. Soc.*, **131**, 16589 (2009).
14. R. A. Van Santen, *Acc. Chem. Res.*, **42**, 57 (2008).
15. G. C. Bond, *Chem. Soc. Rev.*, **20**, 441 (1991).
16. M. Boudart, *Adv. Catal.*, **20**, 153 (1969).
17. S. Melada, F. Pinna, G. Strukul, S. Perathoner and G. Centi, *J. Catal.*, **235**, 241 (2005).
18. J. Park, J. Joo, S. Kwon, Y. Jang and T. Hyeon, *Angew. Chem. Int. Ed.*, **46**, 4630 (2007).
19. K.-S. Kim, N. D. Demberelnyamba, S.-W. Yeon, S. Choi, J.-H. Cha and H. Lee, *Korean J. Chem. Eng.*, **22**, 717 (2005).
20. J.-H. Cha, K.-S. Kim and H. Lee, *Korean J. Chem. Eng.*, **26**, 760 (2009).
21. Q. Liu, J. Baur, R. E. Schaak and J. Lunsford, *Angew. Chem. Int. Ed.*, **47**, 6221 (2008).
22. S.-W. Kim, J. Park, Y. Jang, Y. Chung, S. Hwang, T. Hyeon and Y. W. Kim, *Nano Lett.*, **3**, 1289 (2003).
23. Z. Yang and K. J. Klabunde, *J. Organomet. Chem.*, **694**, 1016 (2009).
24. S. Park, S. H. Lee, S. H. Song, D. R. Park, S. H. Baeck, T. J. Kim, Y. M. Chung, S. H. Oh and I. K. Song, *Catal. Commun.*, **10**, 391 (2009).
25. S. Melada, R. Rioda, F. Menegazzo, F. Pinna and G. Strukul, *J. Catal.*, **239**, 422 (2006).
26. S. Abate, G. Centi, S. Melada, S. Perathoner, F. Pinna and G. Strukul, *Catal. Today*, **104**, 323 (2005).